

**Human Mitochondrial Thymidine Kinase (TK-2) is Selectively Inhibited by 3'-Thiourea Derivatives of  $\beta$ -Thymidine. Identification of residues crucial for both inhibition and catalytic activity\***

**Jan Balzarini, Ineke Van Daele, Ana Negri, Nicola Solaroli, Anna Karlsson, Sandra Liekens, Federico Gago, and Serge Van Calenbergh**

*Rega Institute for Medical Research, Katholieke Universiteit Leuven, Leuven, Belgium (J.B., S.L.); University of Ghent, Ghent, Belgium (I.V.D., S.V.C.); Departamento de Farmacologia, Universidad de Alcalá, Alcalá de Henares, Madrid, Spain (A.N., F.G.); and The Karolinska Institute, Huddinge University Hospital, Huddinge, Sweden (N.S., A.K.)*

Running title page

**Running title:** Inhibition of mitochondrial TK by dThd 3'-thiourea derivatives.

**Address correspondence to:** Jan Balzarini, Rega Institute for Medical Research,  
K.U.Leuven, Minderbroedersstraat 10, B-3000 Leuven, Belgium. Tel: 32-16-337367; Fax: 32-  
16-337340; E-mail: [jan.balzarini@rega.kuleuven.be](mailto:jan.balzarini@rega.kuleuven.be).

Number of text pages: 19

Number of tables: 2

Number of figures: 7

Number of references: 40

Number of words in the Abstract: 246

Number of words in the Introduction: 469

Number of words in the Discussion: 1,487

Abbreviations

TK, thymidine kinase; dTTP, thymidine triphosphate; AZT, 3'-azidothymidine; FIAU, 2'-fluoro-5-iodoarabinosyluracil; ddC, 2',3'-dideoxycytidine; MDS, mitochondrial DNA depletion syndrome; dNTP, 2'-deoxynucleotide 5'-triphosphate; DMF, dimethylformamide; DMSO, dimethylsulfoxide; ATP, adenosine 5'-triphosphate; ADP, adenosine 5'-diphosphate; HSV, herpes simplex virus; VZV, varicella zoster virus; DTT, dithiothreitol; HPLC, high performance liquid chromatography; ITPG, isopropyl-1-thio- $\beta$ -D-galacto-pyranoside; GST, glutathione transferase; BVDU, (*E*)-5-(2-bromovinyl)-2'-deoxyuridine; TMP, thymidylate; TMPKmt, *Mycobacterium tuberculosis*-encoded thymidylate kinase

## ABSTRACT

Substituted 3'-thiourea derivatives of  $\beta$ -thymidine (dThd) and 5'-thiourea derivatives of  $\alpha$ -dThd have been evaluated for their inhibitory activity against recombinant human cytosolic dThd kinase-1 (TK-1), human mitochondrial TK-2, herpes simplex virus type 1 (HSV-1) TK and varicella-zoster virus (VZV) TK. Several substituted 3'-thiourea derivatives of  $\beta$ -dThd proved highly inhibitory to and selective for TK-2 ( $IC_{50}$ : 0.15-3.1  $\mu$ M). The 3'-C-branched *p*-methylphenyl (**1**) and 3-CF<sub>3</sub>-4-Cl-phenyl (**7**) thiourea derivatives of  $\beta$ -dThd showed competitive inhibition of TK-2 when dThd was used as the variable substrate ( $K_i$ : 0.40  $\mu$ M and 0.05  $\mu$ M, respectively) but uncompetitive inhibition in the presence of variable concentrations of ATP ( $K_i$ : 15  $\mu$ M and 2.0  $\mu$ M, respectively). These kinetic properties of **1** and **7** against TK-2 could be accounted for by molecular modeling showing that two hydrogen bonds can be formed between the thiourea nitrogens of **7** and the oxygens of the  $\gamma$ -phosphate of ATP. The importance of several active-site residues was assessed by site-directed mutagenesis experiments on TK-2 and the related HSV-1 TK. The low  $K_i/K_m$  ratios for **1** and **7** (0.38 and 0.039 against dThd, and 0.75 and 0.12 against ATP, respectively) indicate that these compounds are amongst the most potent inhibitors of TK-2 described so far. In addition, a striking close correlation was found between the inhibitory activities of the test compounds against TK-2 and *Mycobacterium tuberculosis* thymidylate kinase that is strongly indicative of close structural and/or functional similarities between both enzymes in relation to their mode of interaction with these nucleoside analogue inhibitors.

## Introduction

The important role of mitochondrial nucleoside kinase TK-2 in mitochondrial homeostasis, including maintenance of the mitochondrial dNTP pools and mitochondrial DNA levels, has become increasingly clear in recent years. Mutations in TK-2 have been described in individuals with a mitochondrial DNA depletion syndrome (MDS) who often develop a devastating myopathy (Saada et al., 2001; Mancuso et al., 2002). Also, long-term use of some antiviral nucleoside analogues such as AZT (zidovudine), FIAU (fialuridine) or ddC (zalcitabine) has been associated with side-effects affecting different organs, such as muscle, liver and/or heart (Lewis et al., 2003; Kohler & Lewis, 2007). It has been suggested that these drug-related toxicities are the consequence of mitochondrial damage due to mitochondrial DNA depletion. This may be caused by chronic inhibition of the TK-2-catalyzed dThd phosphorylation in the mitochondria, which results in dTTP depletion (Lynx & McKee, 2006), but also through inhibition of mitochondrial DNA polymerase  $\gamma$  by some of the drugs (Cherrington et al., 1994; Lim & Copeland, 2001). The design and development of specific TK-2 inhibitors may contribute to the study of the role of TK-2 in different physiological processes that can lead to mitochondrial damage (Pérez-Pérez et al., 2008).

A variety of TK-2 inhibitors have been described in the literature [for an overview, see Pérez-Pérez et al. (2008)], and include 3'-hexanoylamino-dThd (Kierdaszuk et al., 1999), pyrimidine ribofuranosyl nucleosides, 3'-spiroribonucleosides (Balzarini et al., 2000) and arabinosyl nucleosides containing long chain acyl substituents at the C-2' position of the sugar ring (Balzarini et al., 2001; Manfredini et al., 2001; Ciliberti et al., 2007). Interestingly, pyrimidine 2'-deoxynucleoside analogues containing a trityl moiety at the 5'-position of the deoxyribose have also been shown to act as potent and selective inhibitors of TK-2 (Hernández et al., 2002). Further synthetic efforts subsequently led to the identification of, and detailed studies on, tritylated acyclic pyrimidine nucleoside analogues as TK-2 inhibitors (Hernández et al., 2003). These compounds act as non-nucleosidic inhibitors and are endowed with a pronounced inhibitory activity against the enzyme (50% inhibitory concentrations as low as 0.3  $\mu$ M) (Hernández et al., 2002, 2003, 2006; Balzarini et al., 2003; Priego et al., 2004;

Pérez-Pérez et al., 2008). In this study, we report on the discovery of a series of substituted 3'- or 5'-thiourea derivatives of  $\beta$ - and  $\alpha$ -dThd, respectively, as TK-2 inhibitors, and the identification of several derivatives that were highly potent in their anti-TK-2 action. This work also revealed the importance of several active-site residues in TK-2 for inhibition and catalytic activity as well as unexpected similarities in inhibitory potency of these inhibitors against the more distantly related mycobacterial thymidylate kinase.

## MATERIALS AND METHODS

**Compounds.** With the exception of compound **7** and **8**, the chemical synthesis and characterization of the compounds have been described earlier (Van Daele et al., 2007). For the synthesis of compounds **7** and **8**, 3'-amino-3'-deoxythymidine (100 mg, 0.41 mmol) was dissolved in DMF (5 mL). After cooling the solution in an ice-bath, 1.25 eq. of the appropriate iso(thio)cyanate was added and the reaction mixture was allowed to stir at room temperature for 3 h. After reaction completion, the reaction mixture was evaporated to dryness and the residue was purified by column chromatography (CH<sub>2</sub>Cl<sub>2</sub>/MeOH 95:5→90:10) to obtain the desired thiourea and urea analogues IVD914 (**7**) and IVD918 (**8**) in resp. 84 and 81% yield as white powders.

### **1-(3'-deoxy-thymidin-3'-yl)-3-(4-chloro-3-(trifluoromethyl)phenyl)thiourea**

(**compound 7**). <sup>1</sup>H NMR (300 MHz, DMSO-d<sub>6</sub>): δ 1.79 (3H, d, *J*= 0.9 Hz, 5-CH<sub>3</sub>), 2.16-1.2.40 (2H, m, H-2' and H-2''), 3.70 (2H, m, H-5' and H-5''), 3.97 (1H, dd, *J*= 3.3 Hz and 7.5 Hz, H-3'), 4.84 (1H, m, H-4'), 5.17 (1H, s, 5'-OH), 6.24 (1H, app t, *J*= 6.6, H-1'), 7.64 (1H, d, *J*= 8.8 Hz, arom H), 7.72 (1H, dd, *J*= 2.8 and 9.0 Hz, arom H), 7.80 (1H, s, arom H), 8.09 (1H, d, *J*= 0.9 Hz, H-6), 8.61 (1H, br s, C(3')NH), 9.78 (1H, br s, C(3')NHC(S)NH), 11.31 (1H, br s, N(3)H); HRMS (ESI-MS) for C<sub>18</sub>H<sub>19</sub>ClF<sub>3</sub>N<sub>4</sub>O<sub>4</sub>S [M+H]<sup>+</sup> found, 476.0792; calcd, 479.0762.

### **1-(3'-deoxy-thymidin-3'-yl)-3-(4-chloro-3-(trifluoromethyl)phenyl)thiourea**

(**compound 8**). <sup>1</sup>H NMR (300 MHz, DMSO-d<sub>6</sub>): δ 1.79 (3H, d, *J*= 1.2 Hz, 5-CH<sub>3</sub>), 2.12-1.2.33 (2H, m, H-2' and H-2''), 3.63 (2H, m, H-5' and H-5''), 3.54-3.72 (1H, m, H-3'), 4.29 (1H, m, H-4'), 5.09 (1H, t, *J*= 5.4 Hz, 5'-OH), 6.19 (1H, app t, *J*= 6.4, H-1'), 6.89 (1H, d, *J*= 7.5 Hz, arom H), 7.56 (2H, arom H and C(3')NH), 7.77 (1H, d, *J*= 1.2 Hz, arom H), 8.07 (1H, d, *J*= 1.8 Hz, H-6), 8.96 (1H, br s, C(3')NHC(O)NH),

11.29 (1H, br s, N(3)H); HRMS (ESI-MS) for  $C_{18}H_{19}ClF_3N_4O_4$   $[M+H]^+$  found, 463.1053; calcd, 463.1040.

**Cells.** Human lymphocyte CEM cells were cultivated in RPMI-1640 culture medium supplemented with 10% foetal bovine serum, 2 mM L-glutamine and 0.075%  $NaHCO_3$ . Subcultivations were performed twice a week.

**Radiochemicals.** The radiolabeled substrate  $[CH_3-^3H]dThd$  (70 Ci/mmol) was obtained from Moravek Biochemicals (Brea, CA).

**Thymidine Kinase Assay Using  $[CH_3-^3H]dThd$  as the Natural Substrate.** The activity of recombinant TK-1, TK-2, HSV-1 TK and VZV TK and the 50% inhibitory concentration of the test compounds were assayed in a 50  $\mu$ l- reaction mixture containing 50 mM Tris/HCl, pH 8.0, 2.5 mM  $MgCl_2$ , 10 mM dithiothreitol (DTT), 0.5 mM CHAPS, 3 mg/ml bovine serum albumin, 2.5 mM ATP, 1  $\mu$ M  $[methyl-^3H]dThd$  and enzyme. The samples were incubated at 37°C for 30 min in the presence or absence of different concentrations (5-fold dilutions) of the test compounds. At this time point, the enzyme reaction proceeded still linearly. Aliquots of 45  $\mu$ l of the reaction mixtures were spotted on Whatman DE-81 filter paper disks. The filters were washed three times for 5 min each in 1 mM ammonium formate, once for 1 min in water, and once for 5 min in ethanol. The radioactivity was determined by scintillation counting.

To determine the  $K_m$  (for dThd or ATP) and  $K_i$  values (for the inhibitors), varying concentrations of dThd (ranging between 0.4 and 5  $\mu$ M) were used at saturating concentrations of ATP (2.5 mM) or varying concentrations of ATP (ranging between 5 and 100  $\mu$ M) at saturating concentrations of dThd (20  $\mu$ M). The kinetic values were derived from Lineweaver-Burk plots.

**Preparation of Murine Liver Homogenates and Stability Measurements of Test Compounds.** Seven adult NMRI mice (~ 20-22 gram) were anaesthetized with ether, blood was taken by heart puncture, and the mice were subsequently killed by cervical dislocation. Livers were removed and minced with a scissor. The liver pieces were washed twice with cold phosphate-buffered saline (PBS) (6 min centrifugation at 1,200 rpm at 4°C) and divided over

5 tubes (~ 2 ml each) for homogenization in a Precellys-24 homogenizer using glass beads (Bertin Technol, VWR, Haasrode, Belgium). After homogenization, the suspension was centrifuged for 30 min at 13,000 rpm at 4°C to remove the glass beads and small liver pieces, after which the supernatant was centrifuged again at 25,000 rpm during 2 hr at 4°C. Aliquots of this liver extract were then aliquoted and frozen at -80°C until use.

Two hundred µl of liver extract were mixed with 200 µl PBS and 200 µl of test compound (300 µM) to obtain a total volume of 600 µl (100 µM test compound). The reaction mixture was incubated for 0, 20, 40, 60 and 240 minutes at 37°C. At each time point, 100 µl was withdrawn, added to 200 µl cold methanol, centrifuged and the supernatant analysed for compound stability by HPLC (Reverse Phase RP-8 (Lichrocard 125-4), Merck, Darmstadt, Germany). Following gradient was used: 2 min buffer A (acetonitrile) 2% + buffer B (50 mM NaH<sub>2</sub>PO<sub>4</sub> + 5 mM heptane sulfonic acid pH 3.2); 6 min linear gradient to 20% buffer A + 80% buffer B; 2 min linear gradient to 25% buffer A + 75% buffer B; 2 min linear gradient to 35% buffer A + 65% buffer B; 8 min linear gradient to 50% buffer A + 50% buffer B; 10 min same buffer mixture; 5 min linear gradient to 2% buffer A + 98% buffer B; 5 min equilibration at 2% buffer A + 98% buffer B. The compounds **1**, **7** and **8** had retention times of 20.2, 20.7 and 19.4 min, respectively.

**Preparation of Human T-Lymphocyte Extracts and Stability Measurements of Test Compounds.** Human T-lymphocyte CEM cells were grown in RPMI-1640 culture medium in a 1-liter culture bottle to a density of 2 x 10<sup>6</sup> cells/ml. Cells were centrifuged at 1,200 rpm at 4°C for 10 min, washed trice with cold PBS, and resuspended in 20 ml PBS at 100 x 10<sup>6</sup> cells/ml. After 2 rounds of 6 x 20 sec sonication on ice, the cell extract was centrifugated at 13,000 rpm for 30 min at 4°C and the supernatant divided in aliquots of 1 ml and frozen at -80°C until use. Stability of the test compounds was performed as described above for the liver homogenates.

**Uptake of compounds 5 and 8 by CEM cell suspensions.** A variety of one-ml suspensions of 10<sup>7</sup> CEM cells in RPMI-1640 culture medium were prepared and exposed to 100 µM of compounds **5** and **8**. At different time points (15, 30, 45 and 60 min), the cell



suspensions were centrifuged and extensively washed (3 times) with 1 ml RPMI-1640 medium (without serum). The cell pellets were then exposed to 66% cold methanol, and the amount of intracellular test compound was determined using HPLC analysis as described above. It was ascertained that any extracellular compound present in the culture medium was efficiently removed since the supernatant after the last centrifugation step did not contain measurable amounts of the compounds.

**Model Building and Refinement of Human TK-2.** The three-dimensional structure of human TK-2 has not been solved experimentally but a reliable molecular model has been built using a profile-based fold-recognition method (Hernández et al., 2006). A  $Mg^{2+}$ -bound ATP molecule was added to this TK-2 structure and the complex was further refined by remodeling the loop that closes over the reaction substrates using as a template the X-ray crystal structure of human thymidylate kinase cocrystallized with the inhibitor  $P^1$ -(5'-adenosyl) $P^5$ -(5'-(3'-azido-3'-deoxythymidyl))pentaphosphate (PDB code: 1E9A) (Ostermann et al., 2000).

**Docking of a Representative Inhibitor into Human TK-2.** The initial geometry for **inhibitor 7** was generated using suitable fragments from the X-ray crystal structures of methyl 4-(3-methylphenylureido)-5-methoxymethyltetrahydrofuran-2-carboxylate (code BEQNAN in the Cambridge Structural Database, CSD) (Allen, 2002), and dThd as found in the complex with HVS-TK (PDB code: 2VTK). The resulting molecular structure was first refined by means of the semiempirical quantum mechanical program MOPAC (Stewart, 1990), using the AM1 Hamiltonian and PRECISE stopping criteria, and further optimized using the restricted Hartree-Fock (RHF) method and a 6-31G(d) basis set, as implemented in the *ab initio* program Gaussian 03 (Frisch et al., 2003). The calculated wave function was used to obtain electrostatic potential-derived (ESP) charges employing the RESP methodology (Bayly et al., 1993).

A multiple structural alignment (Lupyan et al., 2005) of human TK-2, HSV-TK and human thymidylate kinase provided us with an initial suitable location for both the ATP and the dThd substrates in the active site. The **1** inhibitor was placed in the nucleoside binding site of human TK-2 by superimposing the common thymidine skeleton on the docked dThd.

**Molecular Dynamics Simulations.** The MD simulations were carried out using the AMBER 8.0 suite of programs (Case et al., 2005). The bonded and nonbonded parameters for the **1** ligand were assigned, by analogy or through interpolation, from those already present in the AMBER database, in a way consistent with the second-generation AMBER force field (Cornell et al., 1995). The molecular system consisting of human TK-2, ATP<sup>3-</sup>, Mg<sup>2+</sup>, and **1** was neutralized by the addition of 5 sodium ions (Aqvist, 1990), and immersed in a truncated octahedron of ~6000 TIP3P water molecules (Jorgensen et al., 1983). Periodic boundary conditions were applied and electrostatic interactions were treated using the smooth particle mesh Ewald method (Darden et al., 1993) with a grid spacing of 1 Å. The cut-off distance for the non-bonded interactions was 9 Å. The SHAKE algorithm (Ryckaert et al., 1977) was applied to all bonds and an integration step of 2.0 fs was used throughout. Firstly, solvent molecules and counter-ions were relaxed by energy minimization and allowed to redistribute around the positionally restrained enzyme-inhibitor complex (25 kcal·mol<sup>-1</sup>·Å<sup>-2</sup>) during 50 ps of MD at constant temperature (300 K) and pressure (1 atm). These initial harmonic restraints were gradually reduced in a series of progressive energy minimizations until they were completely removed. The resulting system was heated again from 100 to 300 K during 20 ps and then allowed to equilibrate for 500 ps during which positional restraints (5.0 kcal·mol<sup>-1</sup>) on the protein C $\alpha$  atoms of non-loop regions and distance restraints on the hydrogen bonds between the thymidine moiety and the side chain of Gln110 were used. After this time, the resulting complex was simulated for 10.0 ns in the absence of any ligand restraints although for the first 3.0 ns the restraints on the C $\alpha$  atoms of non-loop regions were maintained. System coordinates were collected every 2 ps for further analysis and the computer graphics program PyMOL (De Lano, 2006) was employed for visualization of structures and trajectories.

**Model Building and Simulation of the Michaelis-Menten Complex for HSV-1 TK.**

The three-dimensional X-ray structures of HSV-1 TK in complex with either ADP and deoxythymidine (PDB id: 2VTK) or ADP and 5-iodo-deoxyuridine-monophosphate (PDB id: 3VTK) (Wild et al., 1997) were used for construction of both the Michaelis-Menten (MM) complex with bound ATP<sup>3-</sup>, a Mg<sup>2+</sup> ion and dThd.

To refine the experimental structure it was necessary to build two missing loops. The Ser149–Pro153 loop was modeled using as a template the crystal structure of HSV–TK complexed with ganciclovir (PDB id: 1KI2, chain B) (Champness et al., 1998). The Gly264–Pro280 loop was built in two steps: first, the Gly264–Val267 and Pro274–Pro280 segments were modeled using as a template the crystal structure of HSV–TK (PDB id: 1E2J, chain B) (Vogt et al., 2000); the remaining loop residues (Pro268–Glu273) were built by satisfaction of spatial restraints using the MODLOOP server (Fiser & Sali, 2003). The resulting MM complex was neutralized, immersed in a water bath, equilibrated and simulated using molecular dynamics for 10 ns. in the absence of any restraints.

**Site-Directed Mutagenesis, Expression and Purification of Wild-Type and Mutant Human TK-2.** Site-directed mutagenesis of *human* TK2 was performed using the QuikChange site-directed mutagenesis kit (Stratagene, Heidelberg, Germany). Primers used for ILE59 to HIS59: 5'-TGTGTCGAGGGCAATCATGCAAGTGGGAAGACG-3' (forward) and 5'-CGTCTTCCCACTTGCATGATTGCCCTCGACACA-3' (reverse); for ILE59 to LEU59: 5'-TGTGTCGAGGGCAATTTAGGCAAGTGGGAAGACG-3' (forward) and 5'-CGTCTTCCCACTTGCTAAATTGCCCTCGACACA-3' (reverse); for ILE59 to VAL59: 5'-TGTGTCGAGGGCAATGTTGCAAGTGGGAAGACG-3' (forward) and 5'-CGTCTTCCCACTTGCAACATTGCCCTCGACACA-3' (reverse); for ILE59 to TYR59: 5'-TGTGTCGAGGGCAATTATGCAAGTGGGAAGACG-3' (forward) and 5'-CGTCTTCCCACTTGCATAATTGCCCTCGACACA-3' (reverse); for TYR99 to PHE99: 5'-CCTCTGGGCCTGATGTTCCACGATGCCTCT-3' (forward) and 5'-AGAGGCATCGTGGAACATCAGGCCAGAGG-3' (reverse). The *human* TK2 mutations were verified by sequence determinations of both strands (MWG Biotech, Ebersberg, Germany). We expressed the *human* TK2 wild-type and mutants in *E. coli* as a fusion protein to glutathione S-transferase. The plasmids were transformed into Rosetta(DE3) (Novagen, Darmstadt, Germany) and single colonies were inoculated into LB medium supplemented with 100 µg/ml ampicillin. The bacteria were grown at 37°C and protein expression was induced at OD<sub>600</sub> ≈ 0.8 with 1 mM isopropyl-1-thio-β-D-galacto-pyranoside (ITGP) for ≈12h at 27°C.

The expressed protein was purified using glutathione-sepharose 4B (Amersham Pharmacia Biotech, Uppsala, Sweden) as described. The purity of the recombinant protein was verified by sodium dodecyl sulfate-polyacrylamide gel electrophoresis (Phast system, Amersham Pharmacia Biotech, Uppsala, Sweden) and the protein concentration was determined with the Bradford Protein Assay (Bio-Rad, Hercules, CA, USA) using bovine serum albumin as the concentration standard.

**Site-Directed Mutagenesis, Expression and Purification of Wild-Type and Mutant HSV-1 TK.** Mutant HSV-1 TK-enzymes (see table) were derived from the TK sequence cloned in pGEX-5X-1 (Amersham Pharmacia Biotech, Uppsala, Sweden) (Degrève et al., 2000) . Site-directed mutagenesis was performed using the QuickChange Site-Directed Mutagenesis Kit (Stratagene, Westburg, Leusden, The Netherlands) as described before (Fetser et al., 1994). The two oligonucleotide primers (Invitrogen Life Technologies, Merelbeke, Belgium) that were used contained the desired mutation at amino acid position 12 and/or 13 of HSV-1 TK. The mutant DNA was transformed into competent E. coli XL-1 blue. Plasmid preparations from ampicillin-resistant colonies were checked by sequencing of the TK gene on an ABI Prism 3100 sequencer (Applied Biosystems, Foster City, CA), using the ABI Prism Big Dye Terminator Cycle Sequencing Ready Reaction Kit (Applied Biosystems) and transfected in E. coli BL21(DE3)pLysS. Transfected bacteria were grown overnight in 2YT medium containing ampicillin (100µg/ml) and chloramphenicol (40µg/ml) and then diluted in fresh medium. After further growth of the bacteria at 27°C (for 5h), isopropyl-β-D-thiogalactopyranoside (Sigma) was added to a final concentration of 0.1mM to induce the production of the GST-TK fusion proteins. After 16h of further growth at 27°C, cells were pelleted and resuspended in lysis buffer (50 mM Tris, pH 7.5, 1mM dithiothreitol, 5mM EDTA, 10% glycerol, 1% Triton X-100, 0.1mM phenylmethylsulfonyl fluoride, and 0.15mg/ml lysosyme) (Göbel et al., 1994). Bacterial suspensions were passed through a SLM Aminco French Pressure Cell Press (Beun de Ronde, La Abcoude, The Netherlands) and ultracentrifuged (20,000 rpm, 4°C, 30min). GST-TK was purified from the supernatant using Glutathione Sepharose 4B (Amersham Pharmacia Biotech) as described by the supplier. The

protein content of the purified fractions was assessed using Bradford reagent (Sigma). The following primers were used: for Pro12Asn: 5' CGG GTT TAT ATA GAC GGT AAC CAC GGG ATG GGG 3'; for His13Ile: 5' GTT TAT ATA GAC GGT CCC ATC GGG ATG GGG AAA ACC 3'; for Pro12Asn/His13Ile: 5' CTG CGG GTT TAT ATA GAC GGT AAC ATC GGG ATG GGG AAA ACC 3'

To create the Pro12Asn/Tyr127Phe, His13Ile/Tyr127Phe and Pro12Asn/His13Ile/Tyr127Phe mutant enzymes, DNA of respectively the Pro12Asn, the His13Ile or the Pro12Asn/His13Ile mutants was used instead of wild-type DNA, together with the mutagenesis primers which contain the Tyr127Phe mutation.

## RESULTS

**Inhibition of Pyrimidine Nucleoside Kinases by Substituted 3'- and 5'-dThd Thiourea Analogues.** The substituted 3'-branched thiourea- $\beta$ -dThd and 5'-thiourea- $\alpha$ -dThd derivatives were synthesized and evaluated for their inhibitory activity against dThd phosphorylation by recombinant purified human cytosolic thymidine kinase-1 (TK-1), human mitochondrial TK-2, herpes simplex virus type 1 (HSV-1) TK and varicella-zoster virus (VZV) TK.

The substituted 3'-branched thiourea- $\beta$ -dThd derivatives (**1-8**) potently inhibited TK-2-catalysed dThd phosphorylation at  $IC_{50}$  values ranging between 0.43 and 3.1  $\mu$ M (Table 1). The anti-TK-2 activity was influenced by the nature of the substituent on the thiourea moiety. The presence of 4-benzyloxyphenyl (**4**), 4-chloro-3-trifluoromethylphenyl (**5**) or 3,4-dichlorophenyl (**6**) moieties on thiourea afforded the best anti-TK-2 activity (Fig. 1, Table 1). **4-6** showed an outstanding selectivity against TK-2 when compared to TK-1 ( $SI \geq 1,000$ ). The promising results obtained with derivative **5** prompted us to synthesize **7**, in which the similar substituted thiourea group is connected directly to the sugar ring (Fig. 1). Such 3'-amino-3'-deoxythymidine derivatives are synthetically more readily accessible than the branched-chain analogues. Surprisingly, with an  $IC_{50}$  value of 0.15  $\mu$ M, analogue **7** surpassed the inhibitory activity of its branched-chain congener **5** whereas the corresponding urea derivative in which the sulfur atom was replaced by an oxygen (**8**) proved to be only slightly less inhibitory against the TK-2 enzyme (Table 1). In contrast, all 3'-thiourea- $\beta$ -dThd analogues (with or without branching) were devoid of inhibitory activity against cytosolic TK-1 at 500  $\mu$ M, that is, at concentrations that are at least 2 to 3 orders of magnitude higher than those required for TK-2 inhibition. Also, they showed poor, if any, inhibitory activity against HSV-1 TK ( $IC_{50}$ :  $46 \geq 500 \mu$ M) and only moderate activity against the closely-related VZV TK ( $IC_{50}$ : 15-77  $\mu$ M) (Table 1). Thus, the 3'-branched thiourea- $\beta$ -dThd analogues showed a surprising specificity for TK-2 when compared with HSV-1 and VZV TK that belong to the same family of enzymes, as well as with the more distantly related TK-1.

The corresponding substituted 5'-thiourea- $\alpha$ -dThd derivatives (**10–16**) were markedly less inhibitory to TK-2 than the substituted 3'-thiourea- $\beta$ -dThd analogues and completely inactive against TK-1 (Table 1). The most potent inhibitors showed an IC<sub>50</sub> that ranged between 31 and 57  $\mu$ M, that is, at least 10- to 100-fold less inhibitory than the 3'-thiourea- $\beta$ -dThd derivatives. They also showed a moderate inhibition of HSV-1 and VZV TK enzymes. The  $\alpha$ -dThd lacking the thiourea group at the 5'-position of the deoxyribose, and thus containing free OH groups at the 3' and 5' positions, had an IC<sub>50</sub> between 34 and 99  $\mu$ M for the investigated nucleoside kinases. Taken together, it is clearly seen that the introduction of selected arylthiourea substituents consistently confers TK-2/TK-1 selectivity.

**Stability Measurements of Compounds 5, 7 and 8 and Uptake into Human T-Lymphocyte CEM Cells.** Compounds **5**, **7** and **8** were examined for their stability in human T-lymphocyte CEM cell extracts and in mouse liver homogenates. It was found that the compounds (examined at 100  $\mu$ M) were fully stable in both CEM cell extracts and mouse liver homogenates when incubated for 20, 40, 60 and 240 minutes at 37°C. No traces of breakdown products could be detected by HPLC analysis of the incubated samples.

Uptake of the test compounds by intact CEM cells was also investigated for compounds **5** and **8**. A comparable and extensive uptake of **5** and **8** by the CEM cells was observed within 15 min (Fig. 2) after which further cellular uptake leveled-off. The efficient uptake of the compounds may be related to their (calculated) lipophilic properties (log *P* ranging between 0.92 and 3.08 using Crippen's fragmentation (Ghose and Crippen, 1987) and between 1.34 and 3.77 using Viswanadhan fragmentation (Viswanadhan et al., 1989).

**Kinetic Properties of 1 and 7 against TK-2.** The mode of inhibitory activity of **1** and **7** against TK-2 was investigated. First, the K<sub>i</sub> value for each compound was determined in the presence of a fixed saturating concentration of ATP and variable concentrations of the dThd substrate. Compounds **1** and **7** inhibited the enzyme in a purely competitive fashion and had K<sub>i</sub> values as low as 0.40 and 0.054  $\mu$ M, respectively (Fig. 3). Their K<sub>i</sub>/K<sub>m</sub> values were markedly lower than 1 (0.38 and 0.039, respectively) pointing to an affinity for the enzyme that largely exceeds the affinity for the natural substrate. Second, the K<sub>i</sub> values of the TK-2 inhibitors were

determined in the presence of a fixed saturating concentration of dThd and variable concentrations of the co-substrate ATP. Compounds **1** and **7** showed  $K_i$  values that were higher (1.5 and 2  $\mu\text{M}$ , respectively) than those observed in the presence of dThd as the variable substrate. The  $K_i/K_m$  values were again lower than 1 (0.75 and 0.12  $\mu\text{M}$ ) (Fig. 3). However, under these conditions, the TK-2 inhibitors behaved kinetically differently and displayed an uncompetitive mechanism of enzyme inhibition, as revealed by the (virtually) parallel kinetic lines in the Lineweaver-Burk plots (Fig. 3). It would also have been interesting to reveal whether compounds **1** and **7** showed uncompetitive kinetics against HSV-1 TK as well in the presence of varying ATP concentrations. However, due to the markedly lower (100- to 1,000-fold) inhibitory activity of these compounds against HSV-1 TK, and their limited solubility at concentrations higher than 500  $\mu\text{M}$ , it was impossible to perform these experiments.

**Molecular Modeling and Computer Simulations.** On the basis of the experimental results, binding of the most potent inhibitor, **7**, to human TK-2 was simulated in the presence of bound ATP. The crucial interactions observed after docking were maintained in the equilibrated complex and some others ensued from the mutual adaptation brought about by the MD procedure. In the final structure (Fig. 4), the **7** ligand appears to be stabilized in the binding site by the following interactions: (i) the thymine moiety of the inhibitor is sandwiched between the phenyl ring of Phe143 on one side and the side chains of both Trp86 and Val115 on the other side, (ii) the thymine O4 and N3 atoms establish good hydrogen bonds with the carboxamide group of Gln110, (iii) the O5' hydroxyl is fixed by the guanidinium nitrogen of Arg134, (iv) the substituted phenyl ring stacks against the side chain of Ile59 and is oriented such that its trifluoromethyl group points to Arg196 and the chlorine atom faces a hydrophobic cavity lined by the side chains of Leu193, Ile204, and Leu209, and, last but not least, (v) both thiourea nitrogens hydrogen bond to the  $\gamma$ -phosphate oxygens of ATP (Fig. 4).

**Construction of mutant TK-2 and herpes simplex virus type 1 TK and susceptibility to the inhibitory activity of **1** and **7**.** Our molecular modeling data suggested that the side



chain of Ile59 in TK-2 stacks against the phenyl ring of **7**. Because the equivalent position in HSV-1 TK and VZV TK, which are much less sensitive to the inhibitors (Table 1) is occupied, respectively, by either a His or a Tyr (Fig. 5) it was then hypothesized that replacement of Ile59 by any of these more polar amino acids, and also by the slightly different but equally hydrophobic Val and Leu, should have an influence on the potency of the inhibitors against TK-2. Consistent with this view, the conservative Ile59Val and Ile59Leu TK-2 mutants showed at least an equal or even a slightly higher (2-fold) sensitivity to the inhibitory activity of **7** and **1** than did wild-type TK-2 enzyme (Table 2). In contrast, the Ile59His and Ile59Tyr TK-2 mutants lost 2- to 3-fold and  $\geq 10$ -fold sensitivity, respectively, to the inhibitory activity of both test compounds (Table 2). Rather unexpectedly, however, it was also noted that these mutations were considerably damaging (Ile59Val and Ile59Leu) or highly detrimental (Ile59His and Ile59Tyr) for the catalytic activity of the mutant TK-2 enzymes, which was decreased to  $\sim 15\%$  or  $\leq 0.05\%$ , respectively, that of the wild-type enzyme. The  $K_m$  values for the natural substrate, on the one hand, were virtually unchanged (3.9-6.0  $\mu\text{M}$ ).

In view of these results we decided to try a reverse approach aimed at increasing the sensitivity to these inhibitors of the more resilient HSV-1 TK. This enzyme has been structurally characterized in atomic detail by X-ray crystallography in complex with a variety of ligands (Wild et al., 1997; Champness et al., 1998; De Lano, 2006). To this end the histidine residue (His13) in HSV-1 TK that occupies a position equivalent to that of Ile59 in TK-2 (Fig. 5) was mutated to isoleucine. The His13Ile HSV-1 TK mutant enzyme turned out to be catalytically virtually inactive and was not inhibited by **7** (Table 2). Because we thought that this outcome could be due to structural rearrangements in the ATP-binding Gly-rich loop that would prevent productive binding of the ATP co-substrate, we probed the effect of replacing the preceding residue (Pro12) with an asparagine, which is the amino acid present in TK-2 in the equivalent position (Asn58) and does not appear to interact directly with the inhibitor according to our model (Fig. 4). The Pro12Asn mutant HSV-1 TK retained  $\sim 10\%$  of the catalytic activity of the wild-type enzyme and both enzymes were inhibited by **7** to a similarly low extent. The additional introduction of this second mutation into the first,

inactive, His13Ile mutant resulted in a further decrease of the catalytic activity (Table 2). Compound **7** was as poor an inhibitor for the His13Ile/Pro12Asn double mutant as it was for the wild-type enzyme. A new attempt to regain activity in the His13Ile mutant HSV-1 TK consisted of introducing another second mutation at the position of the residue that most closely interacts with the side chain of this amino acid, that is, Tyr127, which is positionally equivalent to Phe144 in TK-2. The His13Ile/Tyr127Phe double mutant was active because of improved  $V_{\max}$  and  $K_m$  values relative to the single His13Ile mutant but was still poorly inhibited by **7**. Both the Pro12Asn/Tyr127Phe double mutant and the His13Ile/Pro12Asn/Tyr127Phe triple mutant were catalytically virtually inactive and completely resilient to inhibition by the test compounds (Table 2).

## DISCUSSION

We report here on a novel structural class of compounds that exert a potent inhibitory effect on mitochondrial TK-2. The most potent and selective compound (i.e. **7**) showed a 2,000-fold TK-2 selectivity when compared with cytosolic TK-1 against which it was only marginally inhibitory. Compound **7** is the most potent inhibitor of TK-2, with a  $K_i$  of 0.054  $\mu\text{M}$  and  $K_i/K_m$  of 0.039 when determined against dThd as the natural substrate. Whereas these compounds were found to display purely competitive inhibition kinetics with respect to dThd, the inhibitors showed an uncompetitive kinetic profile against ATP ( $K_i/K_m$  of 0.12 for **7**). In this respect, this class of compounds behaves differently from BVDU, which showed competitive inhibition against dThd but non-competitive inhibition against the co-substrate ATP (Balzarini et al., 2003). Thus, the TK-2 inhibitors herein described most likely occupy (at least partially) the substrate-binding site but only after the co-substrate ATP is bound to the enzyme. In agreement with this line of reasoning, our molecular model revealed a binding mode whose most intriguing feature is the existence of two hydrogen bonds between the thiourea moiety of the **7** inhibitor and the  $\gamma$ -phosphate of ATP. This finding could account for the observed unusual kinetic behavior of this type of compounds against the enzyme. Interestingly, the substituted thiourea dThd analogues kinetically behave like the acyclic 5'-trityl nucleoside analogues earlier described as TK-2 inhibitors (Balzarini et al., 2003; Hernández et al., 2006). Indeed, TK-2 inhibition by such inhibitors (i.e. (*E*)-5-(2-bromovinyl)-1-[(*Z*)-4-triphenylmethoxy-2-butenyl]uracil and 1-[(*Z*)-6-pyridyldiphenylmethoxy)hexyl]thymine) is also competitive with respect to dThd but uncompetitive with respect to ATP. A rationale for these kinetic data was provided by docking some of the representative inhibitors into a homology-based model of TK-2 (Hernández et al., 2006). Our current molecular model can also account for the finding that the 3'-thiourea  $\beta$ -dThd analogues were consistently found to be markedly more inhibitory to TK-2 than the 5'-thiourea  $\alpha$ -dThd congeners. Clearly, subtle differences in the orientation of the deoxyribose

part seem to have a pronounced effect on the eventual affinity and inhibitory activity against TK-2.

Given the high nucleoside kinase selectivity of the reported inhibitors towards TK-2, we attempted to gain insight into the active site amino acids most likely involved in ligand binding by following two alternative and complementary approaches. On the one hand, we mutated Ile59 in TK-2 to several other amino acids (His, Tyr, Val, and Leu) and, on the other hand, we tried to incorporate mutations into HSV-1 TK that would make this enzyme more sensitive to inhibition by these TK-2-selective compounds. Since the molecular modeling results pinpointed a hydrophobic stacking interaction between the substituted phenyl ring of **7** and the side chain of Ile59, we expected weakened ligand binding and partial loss of inhibition for the Ile59His (as in HSV-1 TK) and Ile59Tyr (as in VZV TK) mutant enzymes and no significant differences for the enzymes harboring the more conservative Ile59Val and Ile59Leu mutations. Consistent with this reasoning, the latter mutants were similarly or slightly better inhibited by both **7** and **1** whereas the Ile59His and Ile59Tyr mutant enzymes were less inhibited than wild-type TK-2 (Table 2). What we did not anticipate, however, was the rather drastic loss of catalytic activity that was detected when the kinetic properties of wild-type and mutant enzymes were compared (Table 2).

On the other hand, attempts to make the closely related HSV-1 TK more susceptible to the inhibitory effects of the TK-2-selective compounds by replacing amino acids Pro12 and His13 (X-ray numbering for HSV-1 TK) with their positionally equivalent counterparts in TK-2 (Asn[58] and Ile[59], respectively) were unsuccessful. Furthermore, the catalytic activity of both Pro12Asn and His13Ile mutant enzymes was seriously compromised, particularly in the latter case. When we modeled the Michaelis-Menten complex of the reaction catalyzed by HSV-1 TK we realized that N $\delta$  of His13 forms a good hydrogen bond with the hydroxyl group of Tyr127, which is attached to the phenyl ring that provides the stacking interaction to the pyrimidine ring of dThd in the substrate-binding pocket (Fig. 6). Interestingly, the equivalent residue in TK-2 is a phenylalanine (Phe144), which cannot form such hydrogen bond, but in this enzyme the position of His13 is occupied by Ile59, whose side-chain can establish a

hydrophobic interaction with the phenyl ring of Phe144, according to our model. Because this could be an example of a correlated mutation (Fetser et al., 1994) we thought that the catalytic activity of the His13Ile mutant enzyme would be recovered upon incorporation of a second mutation so as to replace the favorable hydrogen-bonding interaction involving the original His13–Tyr127 couple with an equally favorable hydrophobic interaction between the isoleucine and a phenylalanine, as in the Ile59/Phe144 couple in TK-2 (Fig. 5). This strategy led to a Ile13/Phe127 HSV-1 TK double mutant that was more catalytically active than the single mutants but still more than one order of magnitude less active than wild-type HSV-1 TK (Table 2) and not better inhibited by either **7** or **1**. In view of these results, we tend to think that these mutations preclude proper binding of the ATP molecule and this in turn hampers optimal binding of the inhibitors.

An interesting feature of these thiourea-substituted dThd derivatives is that some of them have recently been reported to inhibit the *Mycobacterium tuberculosis*-encoded thymidylate kinase (TMPKmt) (Van Daele et al., 2007). Nonetheless, whereas the 3'-branched thiourea- $\beta$ -dThd derivatives were superior to the 5'-thiourea- $\alpha$ -dThd derivatives as TK-2 inhibitors, the opposite was true for *M. tuberculosis* TMPK for which the 5'-thiourea- $\alpha$ -dThd analogues were the most active inhibitors (Van Daele et al., 2007). Intriguingly, despite the fact that both enzymes appear to prefer different anomeric configurations of dThd, there is a close correlation between the ranking of the inhibitory potency of these compounds against both enzymes ( $r = 0.89$ ) (Fig. 7). These striking observations may imply that TK-2 and mycobacterial TMPK may be quite similar in terms of interaction kinetics and recognition of modified nucleoside analogue inhibitors at the dThd (in TK-2) and TMP (in TMPKmt) binding sites. In fact, close structural similarities between TK-2 and TMPKmt have been reported recently (Negri et al., 2007) that were rather unexpected in view of the relatively low sequence identity between these enzymes. This structural similarity would account for the unexpected similar susceptibility to several classes of inhibitors and strongly suggests that broader screening assays may be necessary when pursuing high selectivity.

It should be mentioned that the mitochondria represent cellular organelles that are thought to result from prokaryotes that started to live in symbiosis within eukaryotic cells. TK-2 may thus be considered as a prokaryotic-like enzyme similar to the TMPK of *Mycobacterium*. It would therefore be interesting to expand the inhibition studies with these kind of TK-2 inhibitors to other nucleoside or nucleotide kinases of prokaryotic/parasitic origin. Conversely, some acyclic thymidine nucleoside analogues recently reported as potent inhibitors of *Mycobacterium tuberculosis* thymidylate kinase (Familiar et al., 2008) should also be evaluated for their inhibitory potential against TK-2. In fact, it is tempting to speculate that the closely similar kinetic behavior in relation to varying concentrations of either dThd or ATP reported for some 5'-tritylated (a)cyclic-dThd analogues described earlier (Balzarini et al., 2003) and the substituted 3'-thiourea  $\beta$ -dThd analogues delineated herein may reflect a similar mode of interaction with TK-2. It is indeed plausible that the lipophilic trityl group in the 5'-trityl  $\beta$ -dThd analogues and the lipophilic substituted phenyl group present on the thiourea moiety of 3'-thiourea  $\beta$ -dThd derivatives may interact with the same binding site on TK-2. It would thus be very interesting (i) to compare structure-activity data for both groups of compounds against TK-2, (ii) to try to co-crystallize one or more representative compounds with TK-2, and/or (iii) to carry out comparative docking experiments. Efforts in these directions are already underway. In addition, in-depth cell culture studies should also be performed to reveal whether this type of compounds may affect mitochondrial function in intact cells. Although the compounds were chemically and metabolically stable in CEM cell extracts and murine liver homogenates, and extensively taken-up by intact tumor cells, it is currently still unclear whether these compounds are also able to enter the mitochondrial compartment. Further studies will address this issue, and novel thiourea-substituted  $\beta$ -dThd analogues will be designed to specifically target the mitochondria.

In conclusion, we revealed a new class of compounds that are potent inhibitors of TK-2. They have unusual kinetic properties against TK-2 suggesting specific binding of the inhibitors to an enzyme-ATP complex. This kinetic behavior is in agreement with our computer-assisted molecular modeling results. This type of specific TK-2 inhibitors that do

not inhibit cytosolic TK-1 may be useful tools for investigating the mitochondrial depletion syndrome (MDS) that is caused by (partial) TK-2 deficiency and the role of TK-2 in the homeostasis of the mitochondria. The surprising close correlation between the inhibitory activities of the compounds against TK-2 and the distantly-related TMP kinase of *Mycobacterium tuberculosis* is strongly indicative for close structural/functional similarities between both enzymes.

### **Acknowledgments**

The technical assistance of Mrs. Lizette van Berckelaer and Mrs. Kristien Minner and the editorial help of Mrs. Christiane Callebaut is highly appreciated.

## References

- Allen FH (2002) The Cambridge Structural Database: a quarter of a million crystal structures and rising. *Acta Cryst B* **58**: 380-388.
- Aqvist J (1990) Ion–water interaction potentials derived from free energy perturbation simulations. *J Phys Chem* **94**: 8021-8024.
- Balzarini J, Zhu CY, De Clercq E, Pérez-Pérez MJ, Chamorro C, Camarasa MJ, and Karlsson A (2000) Novel ribofuranosyl nucleoside lead compounds for potent and selective inhibitors of mitochondrial thymidine kinase-2. *Biochem J* **351**: 167-171.
- Balzarini J, Degrevè B, Zhu CY, Durini E, Porcu L, De Clercq E, Karlsson A, and Manfredini S (2001) 2'-O-Acyl/alkyl-substituted arabinosyl nucleosides as inhibitors of human mitochondrial thymidine kinase. *Biochem Pharmacol* **61**: 727-732.
- Balzarini J, Hernández AI, Roche P, Esnouf R, Karlsson A, Camarasa MJ, and Pérez-Pérez MJ (2003) Non-nucleoside inhibitors of mitochondrial thymidine kinase (TK-2) differentially inhibit the closely related herpes simplex virus type 1 TK and *Drosophila melanogaster* multifunctional deoxynucleoside kinase. *Mol Pharmacol* **63**: 263-270.
- Bayly CI, Cieplak, P, Cornell WD, and Kollman PA (1993) A well-behave electrostatic potential based method using charge–restraints for deriving charges: The RESP model. *J Phys Chem* **97**: 10269-10280.
- Case DA, Cheatham TE, Darden T, Gohlke H, Luo R, Merz KM, Onufriev A, Simmerling C, Wang B, and Woods RJ (2005) The Amber biomolecular simulation programs. *J Comput Chem* **26**: 1668-1688.
- Champness JN, Bennett MS, Wien F, Visse R, Summers WC, Herdewijn P, De Clercq E, Ostrowski T, Jarvest RL, and Sanderson MR (1998) Exploring the active site of herpes simplex virus type-1 thymidine kinase by X-ray crystallography of complexes with aciclovir and other ligands. *Proteins* **32**: 350-361.
- Cherrington JM, Allen SJ, McKee BH, and Chen MS (1994) Kinetic analysis of the interaction between the diphosphate of (S)-1-(3-hydroxy-2-



- phosphonylmethoxypropyl)cytosine, ddCTP, AZTTP, and FIAUTP with human DNA polymerases beta and gamma. *Biochem Pharmacol* **48**: 1986-1988.
- Ciliberti N, Manfredini S, Angusti A, Durini E, Solaroli N, Vertuani S, Buzzoni L, Bonache MC, Ben-Shalom E, Karlsson A, Saada A, and Balzarini J (2007) Novel selective human mitochondrial kinase inhibitors: design, synthesis and enzymatic activity. *Bioorg Med Chem* **15**: 3065-3081.
- Cornell WD, Cieplak P, Bayly CI, Gould IR, Merz KM, Ferguson DM, Spellmeyer DC, Fox T, Caldwell JW, and Kollman PA (1995) A second generation force field for the simulation of proteins, nucleic acids, and organic molecules. *J Am Chem Soc* **117**: 5179-5197.
- Darden TA, York D, and Pedersen L (1993) Particle mesh Ewald: An N·log(N) method for Ewald sums in large systems. *J Chem Phys* **98**: 10089-10092.
- DeLano W (2006) DeLano Scientific LLC. PyMOL version 0.99. URL: <http://www.pymol.org/>
- Degrève B, Esnouf R, De Clercq E, and Balzarini J (2000) Selective abolishment of pyrimidine nucleoside kinase activity of herpes simplex virus type 1 thymidine kinase by mutation of alanine-167 to tyrosine. *Mol Pharmacol* **58**: 1326-1332.
- Familiar O, Munier-Lehmann H, Negri A, Gago F, Douguet D, Rigouts L, Hernández A-I, Camarasa M-J, and Pérez-Pérez M-J (2008) Exploring acyclic nucleoside analogues as inhibitors of Mycobacterium tuberculosis thymidylate kinase. *Chem Med Chem* **3**: 1083-1093.
- Fetser J, Michael M, Bohner T, Hofbauer R, and Folkers G (1994) A fast method for obtaining highly pure recombinant herpes simplex virus type 1 thymidine kinase. *Protein Expr Purif* **5**: 432-441.
- Fiser A, and Sali A (2003) ModLoop: automated modeling of loops in protein structures. *Bioinformatics* **19**: 2500-2501.

- Ghose AK, and Crippen GM (1987) Atomic physicochemical parameters for three-dimensional-structure-directed quantitative structure-activity relationships. 2. Modeling dispersive and hydrophobic interactions. *J Chem Inf Comput Sci* **27**: 21-35.
- Göbel U, Sander C, Schneider R, and Valencia A (1994) Correlated mutations and residue contacts in proteins. *Proteins* **18**: 309-317.
- Hernández AI, Balzarini J, Karlsson A, Camarasa MJ, and Pérez-Pérez MJ (2002) Acyclic nucleoside analogues as novel inhibitors of human mitochondrial thymidine kinase. *J Med Chem* **45**: 4254-4263.
- Hernández AI, Balzarini J, Rodriguez-Barrios F, San-Félix A, Karlsson A, Gago F, Camarasa MJ, Pérez-Pérez MJ (2003) Improving the selectivity of acyclic nucleoside analogues as inhibitors of human mitochondrial thymidine kinase: replacement of a triphenylmethoxy moiety with substituted amines and carboxamides. *Bioorg Med Chem Lett* **13**: 3027-3030.
- Hernández AI, Familiar O, Negri A, Rodriguez-Barrios F, Gago F, Karlsson A, Camarasa MJ, Balzarini J, and Pérez-Pérez MJ (2006) N1-substituted thymine derivatives as mitochondrial thymidine kinase (TK-2) inhibitors. *J Med Chem* **49**: 7766-7773.
- Jorgensen WL, Chandrasekhar J, Madura JD, Impey RW, and Klein ML (1983) Comparison of simple potential functions for simulating liquid water. *J Chem Phys* **79**: 926-935.
- Kierdaszuk B, Krawiec K, Kazimierczuk Z, Jacobsson U, Johansson NG, Munch-Petersen B, Eriksson S, and Shugar D (1999) Substrate/inhibitor properties of human deoxycytidine kinase (dCK) and thymidine kinases (TK1 and TK2) towards the sugar moiety of nucleosides, including O'-alkyl analogues. *Nucleosides Nucleotides* **18**: 1883-1903.
- Kohler JJ, and Lewis W (2007) A brief overview of mechanisms of mitochondrial toxicity from NRTIs. *Environ Mol Mutagen* **48**: 166-172.
- Lewis W, Day BJ, and Copeland WC (2003) Mitochondrial toxicity of NRTI antiviral drugs: an integrated cellular perspective. *Nature Rev. Drug Discov* **2**: 812-822.
- Lim SE, and Copeland WC (2001) Differential incorporation and removal of antiviral deoxynucleotides by human DNA polymerase gamma. *J Biol Chem* **276**: 23616-23623.

- Lupyan D, Leo-Macías A, and Ortiz AR (2005). A new progressive-iterative algorithm for multiple structure alignment. *Bioinformatics* **21**: 3255-3263.
- Lynx MD, and McKee EE (2006) 3'-Azido-3'-deoxythymidine (AZT) is a competitive inhibitor of thymidine phosphorylation in isolated rat heart and liver mitochondria. *Biochem Pharmacol* **72**: 239-243.
- Mancuso M, Salviati L, Sacconi S, Otaegui D, Camano P, Marina A, Bacman S, Moraes CT, Carlo JR, Garcia M, Garcia-Alvarez M, Monzon L, Naini AB, Hirano M, Bonilla E, Taratuto AL, DiMauro S, and Vu TH (2002) Mitochondrial DNA depletion: mutations in thymidine kinase gene with myopathy and SMA. *Neurology* **59**: 1197-1202.
- Manfredini S, Baraldi PG, Durini E, Porcu L, Angusti A, Vertuani S, Solaroli N, De Clercq E, Karlsson A, and Balzarini J (2001) Design, synthesis and enzymatic activity of highly selective human mitochondrial thymidine kinase inhibitors. *Bioorg Med Chem Lett* **11**: 1329-1332.
- Negri A, Familiar O, Balzarini J, Munier-Lehmann H, Camarasa M-J, Gago F, and Pérez-Pérez M-J (2007) Abstracts of the XV Congreso de la Sociedad Española de Química Terapéutica, San Lorenzo de El escorial, Spain, 11-14 September 2007. Poster no 22. <http://www.seqt.org/seqt/seqt/Libro-Abstracts Escorial.pdf>
- Ostermann N, Lavie A, Padiyar S, Brundiers R, Veit T, Reinstein J, Goody RS, Konrad M, and Schlichting I (2000) Potentiating AZT activation: structures of wild-type and mutant human thymidylate kinase suggest reasons for the mutants' improved kinetics with the HIV prodrug metabolite AZTMP. *J Mol Biol* **1**: 43-53.
- Pérez-Pérez MJ, Priego EM, Hernández AI, Familiar O, Camarasa MJ, Negri A, Gago F, and Balzarini J (2008) Structure, physiological role, and specific inhibitors of human thymidine kinase 2 (TK2): present and future. *Med Res Rev* **28**: 797-820.
- Priego EM, Balzarini J, Karlsson A, Camarasa MJ, and Pérez-Pérez MJ (2004) Non-nucleoside inhibitors of mitochondrial thymidine kinase (TK-2) differentially inhibit the closely related herpes simplex virus type 1 TK and *Drosophila melanogaster* multifunctional deoxynucleoside kinase. *Bioorg Med Chem* **12**: 5079-5090.

- Ryckaert JP, Ciccotti G, and Berendsen HJC (1977) Numerical integration of the cartesian equations of motion of a system with constraints: molecular dynamics of n-alkanes. *J Comput Phys* **23**: 327-341.
- Saada A, Shaag A, Mandel H, Nevo Y, Eriksson S, and Elpeleg O (2001) Mutant mitochondrial thymidine kinase in mitochondrial DNA depletion myopathy. *Nat Genet* **29**: 342-344.
- Stewart JJP (1990) MOPAC: a semiempirical molecular-orbital program. *J Comput Aided Mol Des* **4**: 1-45.
- Van Daele I, Munier-Lehmann H, Froeyen M, Balzarini J, and Van Calenbergh S (2007) Rational design of 5'-thiourea-substituted alpha-thymidine analogues as thymidine monophosphate kinase inhibitors capable of inhibiting mycobacterial growth. *J Med Chem* **50**: 5281-5292.
- Viswanadhan VN, Ghose AK, Revankar GR, and Robins RK (1989) Atomic physicochemical parameters for three dimensional structure directed quantitative structure-activity relationships. 4. Additional parameters for hydrophobic and dispersive interactions and their application for an automated superposition of certain naturally occurring nucleoside antibiotics. *J Chem Inf Comput Sci* **29**: 163-172.
- Vogt J, Perozzo R, Pautsch A, Protá A, Schelling, P, Pilger B, Folkers G, Scapozza L, and Schulz GE (2000) Nucleoside binding site of herpes simplex type 1 thymidine kinase analyzed by X-ray crystallography. *Proteins* **41**: 545-553.
- Wild K, Bohner T, Folkers G, and Schulz GE (1997) The structures of thymidine kinase from herpes simplex virus type 1 in complex with substrates and a substrate analogue. *Protein Sci* **6**: 2097-2106.

## FOOTNOTES

*The authors thank the BOF (Bijzonder Onderzoeksfonds Universiteit Gent, Research Fund Ghent University), the FWO (Fonds voor Wetenschappelijk Onderzoek – Vlaanderen, Fund for Scientific Research – Flanders), the Geconcerteerde Onderzoeksacties Vlaanderen [GOA-05/19], the Spanish Comisión Interministerial de Ciencia y Tecnológica (CICYT) [SAF2006-12713-C02-0], Comunidad de Madrid [BIPEDD-CM, S-BIO/0214/2006] and the Swedish Medical Research Council for financial support of this research.*

## FIGURE LEGENDS

**Fig. 1.** Structural formulae of TK-2 inhibitors and the 50% inhibitory concentration values for TK-2 using dThd as the substrate.

**Fig. 2.** Uptake of compounds **5** and **8** by T-lymphocyte CEM cells. CEM cell suspensions were exposed to 100  $\mu$ M test compound and uptake of compound into the cells at different time points was measured after centrifugation and extensive washing of the cells to remove extracellular compound.

**Fig. 3.** Kinetics of **1** and **7** against purified recombinant mitochondrial TK-2. Lineweaver-Burk plots (1/substrate *versus* 1/velocity) are shown for the inhibition of TK-2 by compound **1** (Panels A, B) and compound **7** (Panels C, D) against dThd (Panels A, C) and ATP (Panels B, D) as the competing substrate.

**Fig. 4.** Proposed binding mode for the best inhibitor, (**7**) (designated IVD 914) (C atoms in white), in the active site of human TK-2 (pink ribbon). ATP is shown as sticks, with C atoms colored in olive green, and  $Mg^{2+}$  is displayed as a sphere colored in magenta. Note the “open” conformation of the loop that normally closes over the reaction substrates. Protein side-chains relevant to the discussion are labeled and shown as sticks except for those of Trp86 and Val115 which have been omitted to improve clarity. Dashed lines represent hydrogen bonds between the thiourea nitrogens and the oxygens of the  $\gamma$ -phosphate of ATP, and between the amide of Q110 and thymine.

**Fig. 5.** Alignment of the 55-65 amino acid stretch in TK-2, HSV-1 TK, VZV TK and TK-1. The amino acids that were mutated in TK-2 and HSV-1 TK are indicated in bold.

**Fig. 6.** View of the active site of HSV TK (grey ribbon) as seen in the simulated Michaelis-Menten complex. ATP and dThd are shown as sticks with C atoms colored in white and pink, respectively, and  $Mg^{2+}$  is displayed as a sphere colored in magenta. Dashed lines represent hydrogen bonds between relevant residues discussed in the text.

**Fig. 7.** Correlation between the  $IC_{50}$  values of the inhibitors against TK-2 and their  $K_i$  values against TMPKmt. The  $K_i$  values were taken from Van Daele et al. (2007). The numbering corresponds to the compound numbers depicted in Fig. 1.

**Table 1.** Inhibitory activity of 3'- and 5'-thiourea derivatives of thymidine against nucleoside kinase-catalysed phosphorylation of 1  $\mu$ M [CH<sub>3</sub>-<sup>3</sup>H]thymidine

Compound	IC <sub>50</sub> <sup>a</sup> ( $\mu$ M)			
	TK-1	TK-2	HSV-1 TK	VZV TK
<b>1</b>	> 500	1.2 $\pm$ 0.1	444 $\pm$ 18	37 $\pm$ 2.0
<b>2</b>	> 500	3.1 $\pm$ 0.3	$\geq$ 500	77 $\pm$ 51
<b>3</b>	> 500	1.2 $\pm$ 1.1	400 $\pm$ 54	31 $\pm$ 5.0
<b>4</b>	$\geq$ 500	0.43 $\pm$ 0.04	232 $\pm$ 39	28 $\pm$ 1.0
<b>5</b>	$\geq$ 500	0.47 $\pm$ 0.04	46 $\pm$ 4.0	21 $\pm$ 5.0
<b>6</b>	$\geq$ 500	0.64 $\pm$ 0.31	87 $\pm$ 36	15 $\pm$ 1.0
<b>7</b>	316 $\pm$ 1.2	0.15 $\pm$ 0.01	195 $\pm$ 54	24 $\pm$ 3.0
<b>8</b>	416 $\pm$ 6.0	0.42 $\pm$ 0.0	335 $\pm$ 25	5.6 $\pm$ 0.8
<b>9</b> ( $\alpha$ -dThd)	99 $\pm$ 51	46 $\pm$ 2.0	34 $\pm$ 3.0	47 $\pm$ 3.0
<b>10</b>	> 500	57 $\pm$ 20	422 $\pm$ 6.0	30 $\pm$ 7.0
<b>11</b>	> 500	405 $\pm$ 78	> 500	40 $\pm$ 3.0
<b>12</b>	> 500	41 $\pm$ 3.0	365 $\pm$ 22	45 $\pm$ 6.0
<b>13</b>	> 500	38 $\pm$ 1.0	472 $\pm$ 40	40 $\pm$ 4.0
<b>14</b>	> 500	110 $\pm$ 13	> 500	95 $\pm$ 66
<b>15</b>	> 500	99 $\pm$ 36	> 500	150 $\pm$ 38
<b>16</b>	> 500	31 $\pm$ 6.0	392 $\pm$ 8.0	45 $\pm$ 1.0

<sup>a</sup>IC<sub>50</sub> is the 50% inhibitory concentration of the test compounds required to inhibit 1  $\mu$ M [CH<sub>3</sub>-<sup>3</sup>H]dThd phosphorylation by 50%.

Data are the mean of 2 to 3 independent experiments.

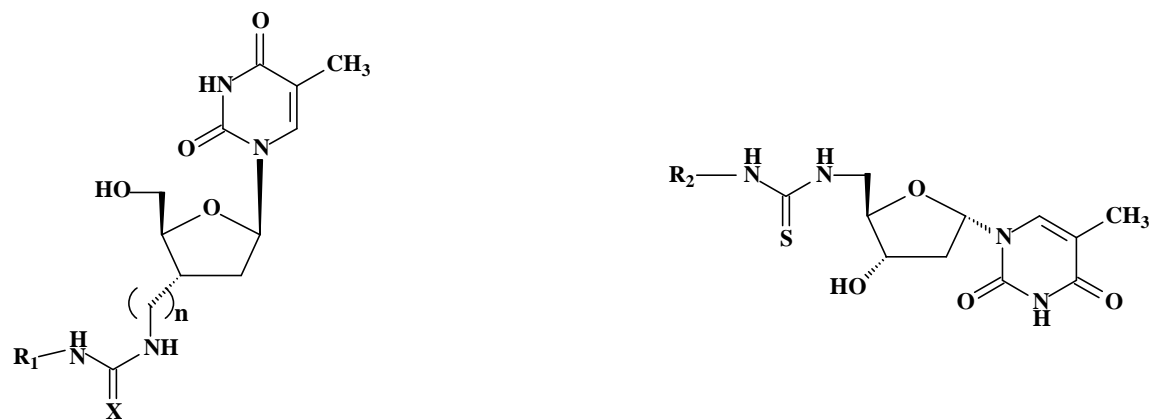


**Table 2.** Kinetic parameters for, and inhibitory activity of test compounds against wild-type and mutant TK-2 and HSV-1 TK

	Compound IC <sub>50</sub> <sup>a</sup>		K <sub>m</sub> (dThd)	V <sub>max</sub>	V <sub>max</sub> /K <sub>m</sub>
	(μM)		(μM)	(pmol/μg/hr)	
	Compound 1	Compound 7			
<u>TK-2</u>					
WT	1.3 ± 0.59	0.15 ± 0.06	4.3 ± 2.3	1956 ± 448	455
Ile59Val	0.61 ± 0.04	0.078 ± 0.011	5.1 ± 1.8	328 ± 59	64
Ile59Leu	1.4 ± 0.75	0.074 ± 0.007	5.6 ± 5.0	322 ± 110	57
Ile59His	6.1 ± 2.0	0.31 ± 0.01	6.0 ± 2.4	1.2 ± 0.0	0.20
Ile59Tyr	> 10	1.8 ± 0.50	3.9 ± 2.4	0.60 ± 0.05	0.15
<u>HSV-1 TK</u>					
WT	> 100	83 ± 11	0.44 ± 0.17	25,667 ± 13,577	58,334
Pro12Asn	> 100	57 ± 23	3.9 ± 1.3	3,000 ± 424	769
His13Ile	> 100	> 100	612 ± 78	607 ± 26	0.99
Pro12Asn + His13Ile	> 100	72 ± 40	0.23 ± 0.042	25 ± 2.1	109
Pro12Asn/Tyr127Phe	> 100	> 100	590 ± 581	490 ± 250	0.83
His13Ile/Tyr127Phe	> 100	87 ± 9.2	37 ± 23	1,389 ± 393	37
Pro12Asn/His13Ile/Tyr127Phe	> 100	> 100	263 ± 194	32 ± 14	0.12

<sup>a</sup>50%-inhibitory concentration required to inhibit enzyme-catalysed dThd (1 μM) phosphorylation by 50%.

Data are the mean of 2 (for TK-2) and 2 to 3 (for HSV-1 TK) independent experiments.



Compound code	X	n	R1	IC <sub>50</sub> (μM) for TK-2	Compound code	R2	IC <sub>50</sub> (μM) for TK-2
1	S	1		1.2	10		57
2	S	1		3.1	11		405
3	S	1		1.2	12		41
4	S	1		0.43	13		38
5	S	1		0.47	14		110
6	S	1		0.64	15		99
7	S	0		0.15	16		31
8	O	0		0.42			

Fig. 1

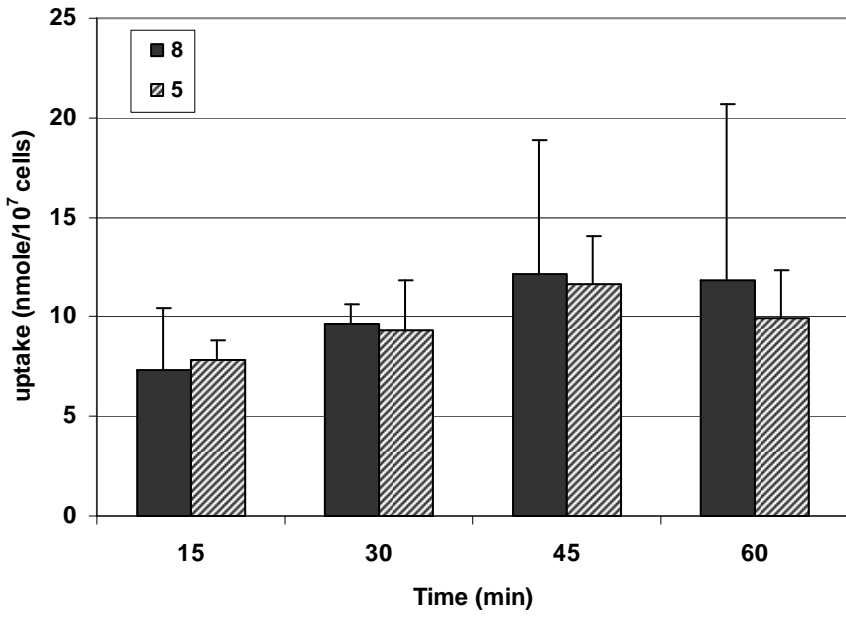


Fig. 2

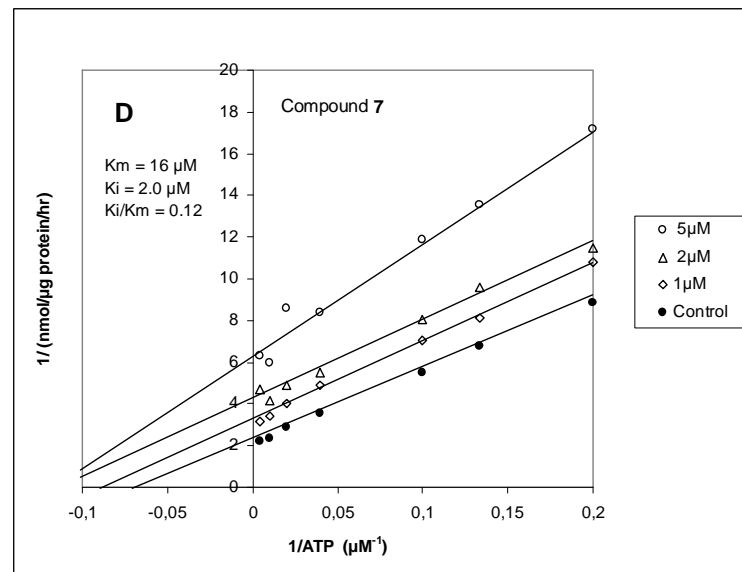
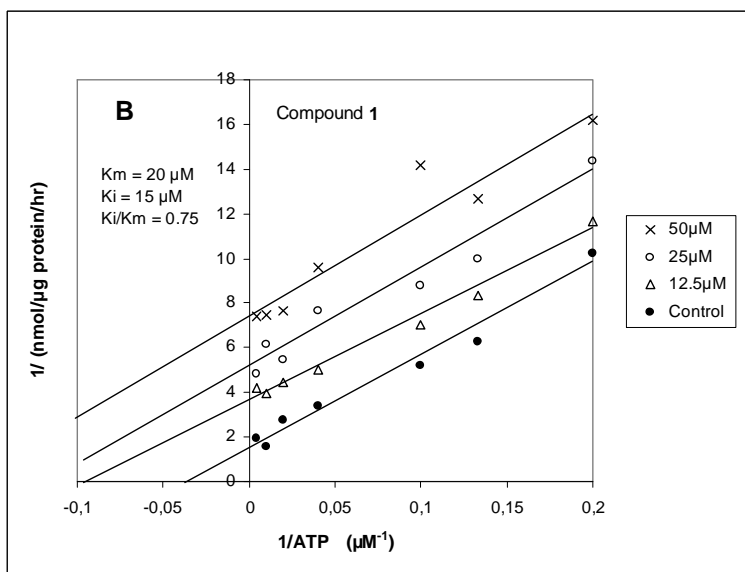
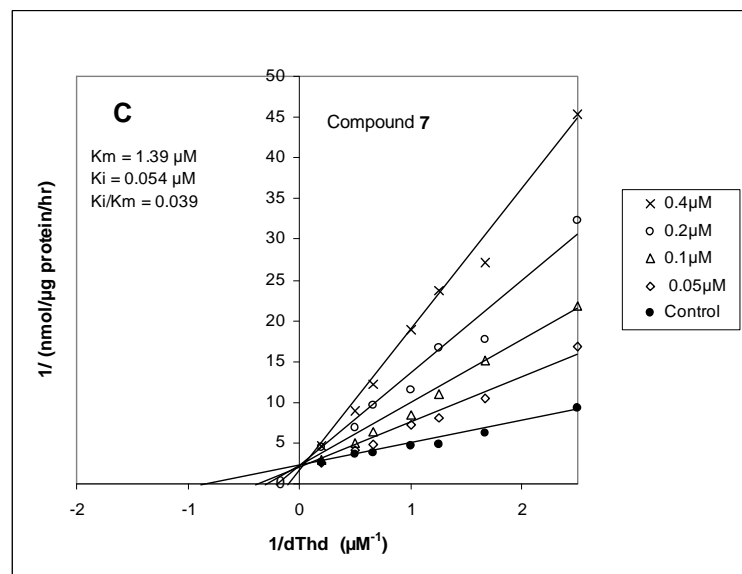
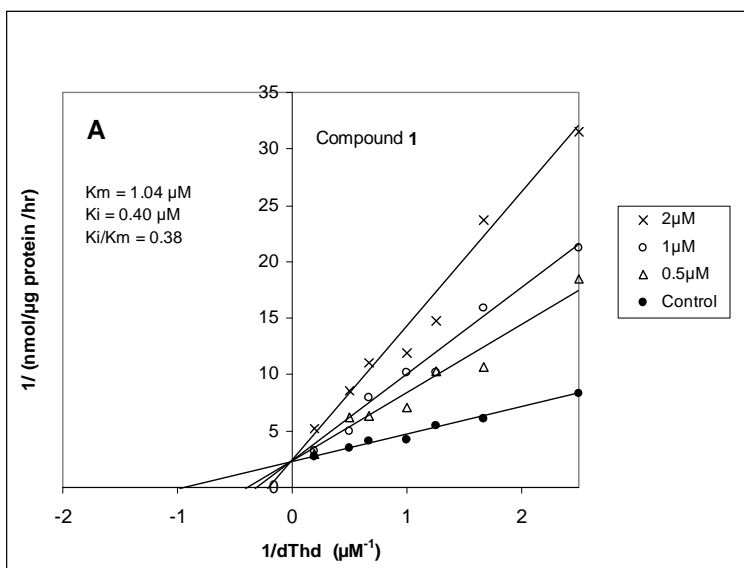


Fig. 3

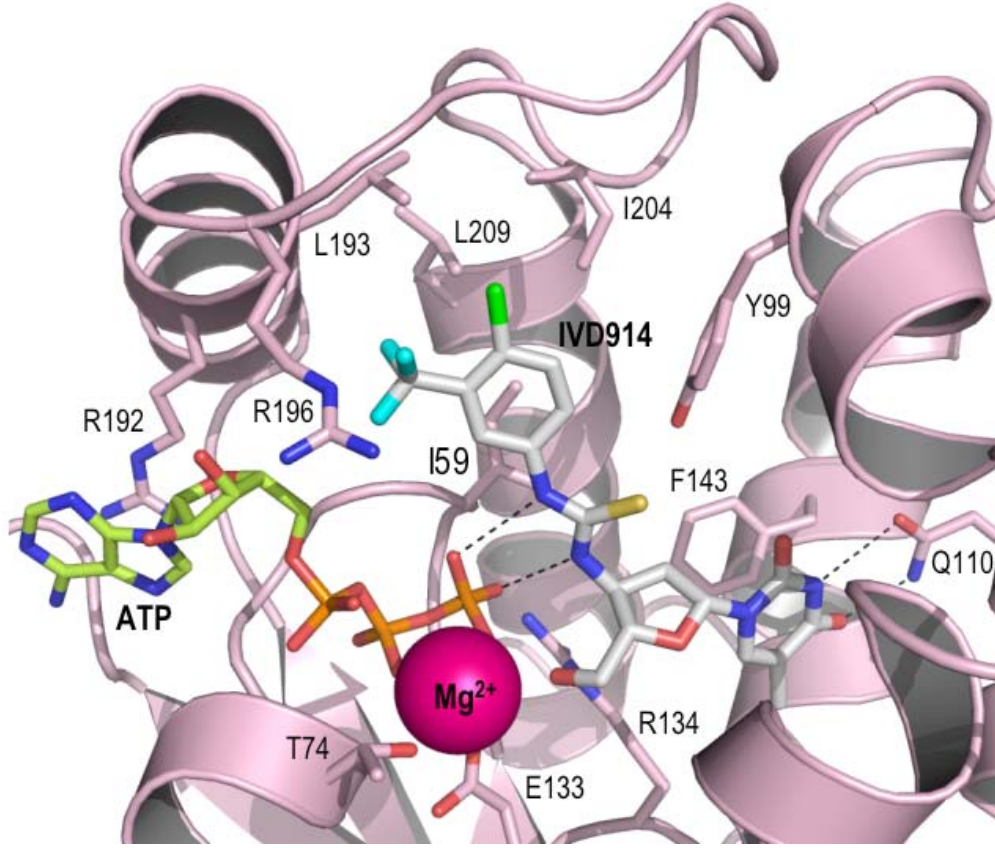


Fig. 4

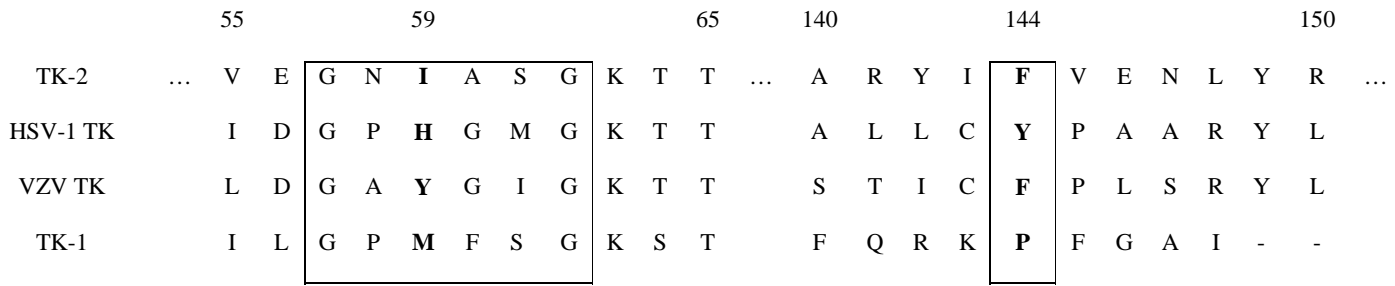


Fig. 5

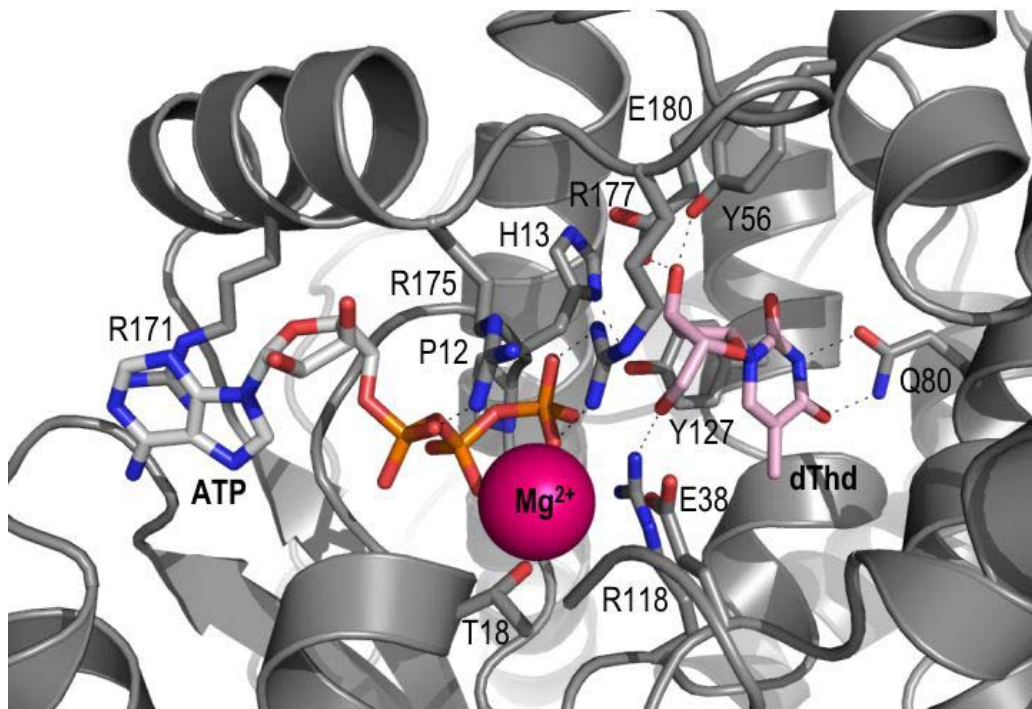


Fig. 6

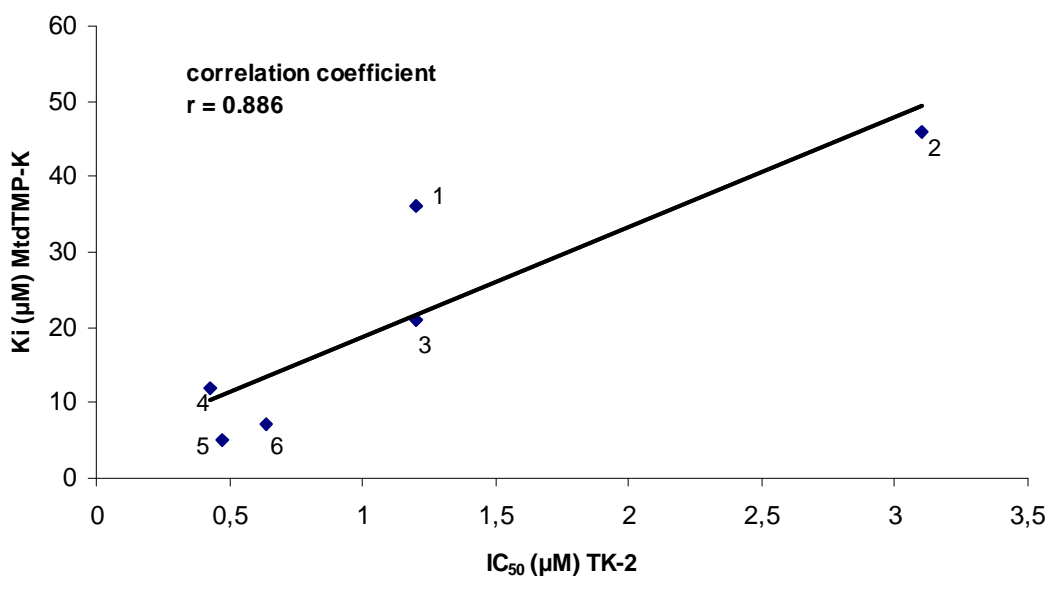


Fig. 7